Fully dynamic stability analysis of jointed rock slopes

Yossef H. Hatzor

Dept. of Geological and Environmental Sciences,
Ben-Gurion University, Beer-Sheva, 84105, Israel

ABSTRACT: A fully dynamic, two dimensional, stability analysis of a highly discontinuous rock slope is demonstrated in this paper. The studied rock slope is the upper terrace of King Herod's Palace in Masada, situated on the western margins of the seismically active Dead Sea Rift. The dynamic deformation of the slope is calculated using a fully dynamic version of DDA in which time dependent acceleration is used as input. The analytically determined failure modes of critical keyblocks in the jointed rock slope are clearly predicted by DDA at the end of the dynamic calculation. It is found however that for realistic displacement estimates some amount of energy dissipation must be introduced into the otherwise fully elastic, un-damped, DDA formulation. Comparison of predicted damage with actual slope performance over historic time span window of 2000 years allows us to conclude that introduction of 2% kinetic damping should suffice for realistic damage predictions. This conclusion is in agreement with recent results of Tsesarsky, Hatzor and Sitar (2002) who compared displacements of a single block on an inclined plane subjected to dynamic loading obtained by DDA and by shaking table experiments. Using dynamic DDA it is shown that introduction of a simple rock bolting pattern completely stabilizes the slope.

RÉSUMÉ : On présente dans cet article une analyse bidimensionnelle complète de la stabilité d'une pente rocheuse très fracturée. La pente rocheuse étudiée est la terrasse supérieure du Palais du roi Hérode à Massada, située sur la rive Ouest du Rift sismiquement actif de la Mer Morte. La pente est constituée de blocs de dolomite raide présentant une stratification sub-horizontale et des joints sub-verticaux. La déformation dynamique de la pente est calculée en utilisant une version entièrement dynamique de l'Analyse de Déformation Discontinue (DDA) où l'accélération dépendant du temps est utilisée comme donnée. Les modes de rupture déterminés analytiquement des blocs clés dans la pente rocheuse fracturée sont clairement prévus par l'approche DDA à la fin du calcul dynamique. On trouve cependant, que pour obtenir des estimations réalistes du déplacement, il faut introduire un facteur de dissipation énergétique sans lequel la formulation DDA serait totalement élastique et sans amortissement. En comparant l'endommagement prévu avec les caractéristiques de la pente sur une période historique de 2000 ans, nous pouvons conclure que l'introduction d'un amortissement cinématique de 2% suffit pour obtenir de prévisions réalistes. Cette conclusion est conforme aux résultats récents de Tsesarsky, Hatzor and Sitar (2002) qui ont comparé les déplacements d'un bloc isolé sur un plan incliné sous chargement dynamique obtenus avec l'analyse DDA et à partir d'essais sur table vibrante.

ZUSAMMENFASSUNG: En utilisant une modélisation DDA dynamique on montre que l'introduction d'un système simple de boulonnage stabilise la pente.In dieser Veroeffentlichung wird eine vollstaendig dynamische, zweidimensionale Stabilitaetsanalyse eines hoechst diskontinuierlichen Steinhangs dargestellt. Der untersuchte Hang ist die obere Terrasse des Herodespalastes in Massada, welche in den westlichen Randgebieten des seismisch aktiven Toten Meer Grabens liegt.Die dynamische Deformation des Berghangs wird mit Hilfe einer vollstaendig dynamischen DDA-Version berechnet, in welcher als Input die zeitabhaengige Beschleunigung eingegeben wird. Die analytisch bestimmten Versagensarten kritischer Schluesselbloecke in diesem zerkluefteten Steinhang werden durch Anwendung von DDA am Ende der dynamischen Berechnung klar vorausgesagt. Es zeigt sich jedoch, dass fuer realistische Dislozierungs-Abschaetzungen ein gewisses Mass an Energieverlust in der sonst vollstaendig elastischen, ungedaempften DDA-Fassung einbezogen werden muss. Der Vergleich des vorhergesagten Schadens mit dem aktuellen Verhalten des Berghangs waehrend einer historischen Zeitspanne von 2000 Jahren erlaubt uns zu schliessen, dass ein Zusatz von 2% kinetischer Daempfung fuer eine realistische Vorhersage des Schadens ausreichen sollte. Diese Schlussfolgerung steht im Einvernehmen mit neuen Ergebnissen von Tsesarsky, Hatzor und Sitar (2002), welche die Dislozierung eines einzelnen Blocks auf geneigter Ebene unter dynamischer Belastung – unter Anwendung von DDA und "shaking table"-Versuchen – verglichen. Mit Hilfe der dynamischen DDA wird gezeigt, dass der Steinhang durch Anwendung einer einfachen Steinschraubenstruktur vollkommen stabilisiert werden kann.

Introduction

In this paper we apply fully dynamic discontinuous deformation analysis (Shi, 1993) to a real jointed rock slope which has sustained a relatively well known record of earthquakes over the past 2000 years – the upper terrace of King Herod's Palace in Masada, situated along the western margins of the seismically active Dead Sea rift valley. Since we know the terrace has sustained tremors of known magnitude in documented historic events we have a good constraint on dynamic DDA predictions, from the field. In particular, the amount of required energy dissipation in DDA, or "damping", can be explored by comparing DDA predictions with actual terrace performance over historic times. Thus, the amount of energy dissipation associated with shaking of a real jointed rock slope may be estimated, and the appropriate values can be used for realistic dynamic modeling of jointed rock slopes using DDA.

In this research a new C/PC version of DDA is used (Shi, 2001) where earthquake acceleration can be input directly in every time step. A necessary condition for direct input of earthquake acceleration is that the numerical computation has no artificial damping, because damping may reduce the earthquake dynamic energy thus under estimating the damage. In DDA the solution of the equilibrium equations is performed without damping and therefore DDA should be a suitable method for the task of a fully dynamic analysis in jointed rock masses. Nevertheless, as will be discussed below, we suggest here that some amount of energy dissipation must be introduced into the otherwise fully un-damped formulation of DDA, if realistic displacement predictions are sought.

Dynamic DDA validation using analytical solutions

Before we attempt to apply dynamic DDA to the full-scale problem of a jointed rock slope it is necessary to check whether dynamic DDA displacements are matched by analytical solutions. Hatzor and Feintuch (2001) demonstrated the validity of DDA results for fully dynamic analysis of a single block on an incline subjected to dynamic loading. A good agreement between the analytical solution and DDA was obtained in all cases (see example in Figure 1 for the function $a_t = 2\sin t + 3\sin 3t$).
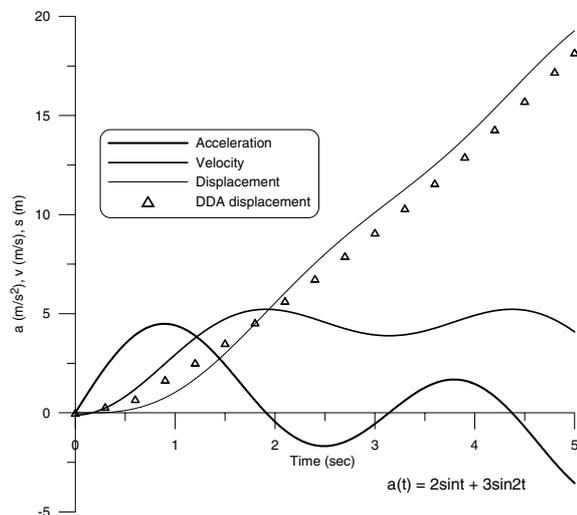

Figure 1: Validation of dynamic DDA for a block on an incline problem (after Hatzor and Feintuch, 2001).

Dynamic DDA validation using shaking table experiments

Wartman (1999) studied the dynamic displacement problem of a block on an incline using shaking table experiments. Following Wartman (1999) Tsesarsky et al. (2002) repeated identical tests numerically using DDA. A representative result is shown in Figure 2 for a sinusoidal input function with frequency of 2.66Hz and interface friction angle of 16°. The DDA output is shown in symbols for four values of energy dissipation (k01): 0%, 1.5%, 2%, and 2.5%. For 0% dissipation (k01 = 1.0) the velocity of each block at the end of a time step is completely transferred to the beginning of the following time step. For 1.5% dissipation (k01=0.985) the velocity at the beginning of a time step is 1.5% smaller than the velocity at the end of the previous time step.

The results of Tsesarsky et al. show that with zero energy dissipation (k01 = 1.0) DDA results overestimate the physical displacements by as much as 80%. With as little as 2% dissipation however (k01=0.98) DDA displacements match the physical test results within 5% accuracy. This finding suggests that realistic application of dynamic DDA must incorporate some energy dissipation in order to account for energy loss mechanisms that are not modelled by DDA. Examples for such energy dissipation mechanisms may be block fracture at contact points, contact surface damage during slip, etc.
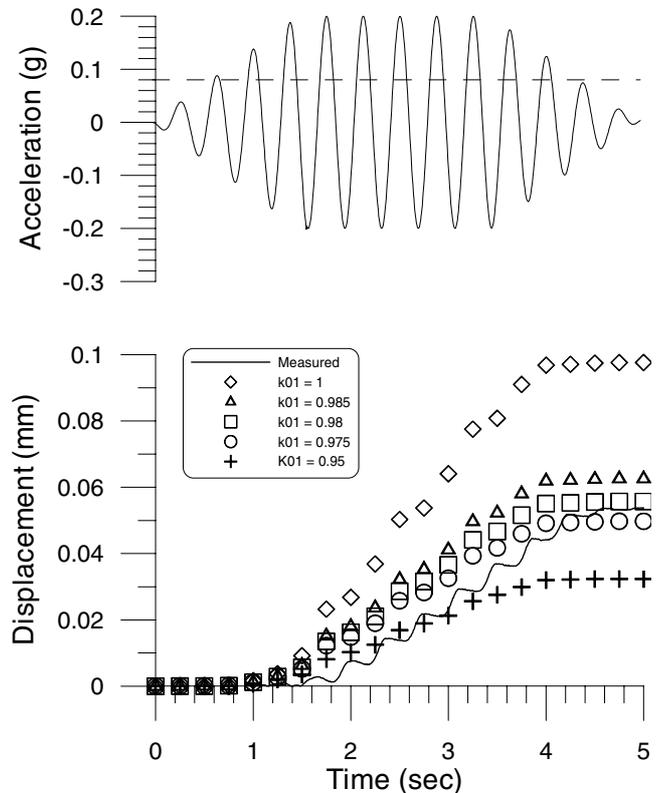

Figure 2: Validation of dynamic DDA using shaking table experiments (After Tsesarsky et al., 2002). Top – sinusoidal input motion, Bottom – comparison between DDA and experiment.

The shaking table validation (Figure 2) pertains to a single block on an incline. McBride and Scheele (2001) studied a multi-block toppling problem using a slope with a stepped

base consisting of 50 blocks. Their conclusion was that as much as 20% energy dissipation was required in order to obtain realistic agreement between the physical model and DDA. Perhaps better conditioning of their numeric control parameters would have reduced the required amount of energy dissipation.

Geological and Seismological Setting Of Herod's Palace, Masada

The top of Mount Masada consists of essentially bare hard rock. The rock is mainly bedded limestone and dolomite, with near vertical jointing. Structurally, the entire mountain is an uplifted block within the band of faults which forms the western boundary of the Dead Sea Rift, a seismically active transform. A review of the tectonics and seismicity of the area is provided by Niemi et al. 1997. According to the Israel building code – Israel Standard 413 the Dead Sea valley has been classified as a region in which earthquake-induced peak horizontal ground acceleration (PGA) exceeding 0.2g at the bedrock level is expected with a 10% probability within any 50 year window. This is analogous to a 475-year average recurrence interval for such acceleration. In this paper we repeatedly refer to PGA for simplicity, which is adequate in the present context, although PGA is not necessarily the best measure of the seismic hazard.

Inspection of the historic earthquake record (e.g. Ben- Menahem, 1979) suggests that the strongest shaking events which have actually affected Mount Masada within the past two thousand years, were due to about ten identified earthquakes with estimated magnitudes in the range of 6.0±0.4 and focal distances probably in the order of several kilometers to a few tens of kilometers from the site. With these parameters, it is highly likely that some of these earthquakes have caused at Mount Masada bedrock PGA's reaching and even exceeding 0.2g, in general agreement with predictions for a 2000 year period based on the aforementioned building code assumptions.

One of the most notable historic earthquakes in this region occurred probably in the year 362 or 363, with a magnitude estimated at 6.4 or even 7.0. Reported effects included seismic seiches in the Dead Sea and destruction in cities tens of kilometers from the Dead Sea both east and west. This is probably the earthquake identified by archeologists as "the great earthquake which destroyed most of the walls on Masada sometime during the second to the fourth centuries" (Netzer, 1991). The most recent of the major historic earthquakes near Mount Masada occurred on July 11th, 1927. This earthquake was recorded by tens of seismographs, yielding a magnitude determination of 6.2 and an epicenter location 30±10 km north of Masada. It also caused a seismic seiches in the Dead Sea and destruction in cities tens of kilometers away (Shapira and Van Eck., 1993).

Observed historical stability

The fortifications built by King Herod on Mount Masada about two thousands years ago included a casemate wall surrounding the relatively flat top of the mountain. Clearly, because of its defensive function, the outer face of this wall was built so as to continue upward the face of the natural cliff, as much as possible. The outer wall was therefore founded typically on the flat top within several decimeters from its rim. Locally it was even founded slightly beyond the rim, on a somewhat lower ledge of rock. On the three palace terraces (Figure 3), jutting at the northern tip of the mountain top, construction was again carried out up to the rim and beyond in order to achieve architectural effects and utilize fully the limited space. Thus, the remaining foundations effectively serve to delineate the position of the natural rim of the flat mountaintop and associated northern terraces about 2000 years ago. Missing portions along such foundation lines indicate locations in which the rim has most probably receded due to rockfalls, unless the portions are missing due to other obvious reasons such as local erosion of the flat top by water or an apparent location of the foundation on fill beyond the rim.

Our inspection of the entire rim of the top of Masada reveals that over almost the entire length of the casemate wall, which is about 1400m, the rock rim has not receded during the past two thousand years more than a few decimeters, if at all. Only over a cumulative total of less

Figure 3: King Herod's palace – Masada. Top - The three terraces of the palace (courtesy of Albatross Inc., Israel). Bottom - A close up view of the upper terrace modeled here.

than 40m, i.e. about 3% of the wall length, there are indications of rockfalls involving rim recessions exceeding 1.5m, but not exceeding 4.0m. Since the height of the nearly-vertical cliffs below the rim is in the order of tens of meters, these observations attest to remarkable overall stability in the face of the recurring earthquakes.

On King Herod's palace terraces there has been apparent widespread destruction, mostly of walls and fills which were somehow founded on the steep slopes. However, in the natural cliffs themselves there are few indications of rockfalls involving rim recessions of more than a few decimeters. Remarkably, most of the high retaining walls surrounding the middle and lower terraces are still standing, attesting to the stability of the rock behind them. In the upper terrace, on which this study is focused, there appears to be only one rockfall with depth exceeding several decimeters. It is a local rockfall near the top of the 22m cliff, in the northeast, causing a rim recession of about 2.0m. It is notable that this particular section of the terrace cliff was substantially modified by the palace builders, perhaps de-stabilizing the pre-existing natural cliff.

We have also inspected rare aerial photographs of Mount Masada dated December 29th 1924, i.e. predating the 1927 earthquake. Our comparison with recent aerial photographs would have been capable of detecting rim recessions exceeding about one meter, if any had occurred in the northern part of the mountain. None were found, suggesting that the 1927 earthquake did not cause any significant rockfalls there (the southern part was less clear in the old photographs).

The information presented above essentially constitutes results of a rare rock-mechanics field-scale "experiment". Two thousand years ago the Masada cliff top was marked by construction. The mountain was later shaken by several major earthquakes, with deep bedrock accelerations certainly exceeding 0.1g and probably even exceeding 0.2g. Observations at the present stage of the "experiment" show that all the cliffs surrounding the top of

Mount Masada essentially withstood the shaking, with some relatively minor rockfalls at the top of the cliffs.

The above is a substantial result of a full-scale "experiment" on the real rock structure. Therefore, a fundamental test of any model of this structure is that it must essentially duplicate the above "experiment". As shown in the sequel, we subjected our DDA model to this test, obtaining instructive results.

Mechanical Properties

The rock in Masada is a massive and dense dolomite with low porosity (2% - 8%) and density of 2,730 kg/m^3. The rock mass is bedded with local karstic voids between beds. The bedding planes are generally clean and tight, with crashed dolomite infilling in places.

Rock Mass Structure

Herod's palace, also known as the North palace, is built on three terraces at the north face of Masada (Figure 3). The rock mass structure at the foundations consists of two orthogonal, sub vertical, joint sets striking roughly parallel and normal to the NE trending axis of the mountain, and a set of well developed bedding planes gently dipping to the north. The joints are persistent, with mean length of 2.7 m. The bedding planes, designated here as J_1, dip gently to the north with mean spacing of 60 cm. The two joint sets, J_2 and J_3, are closely spaced with mean spacing of 14 cm and 17 cm respectively (Figure 4).
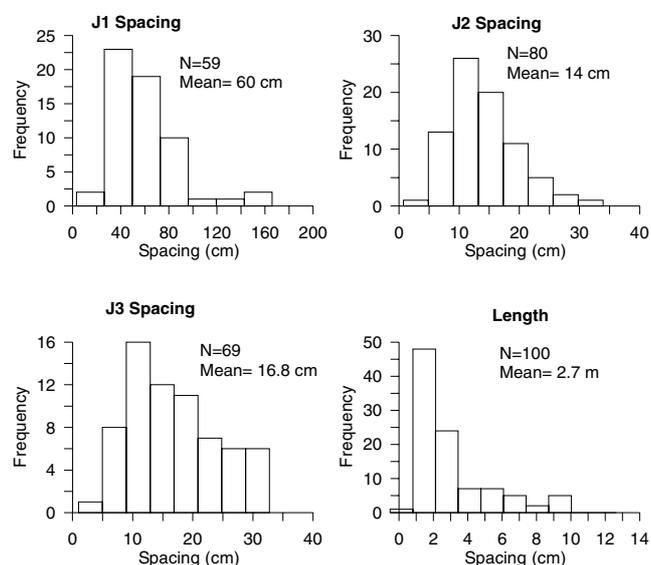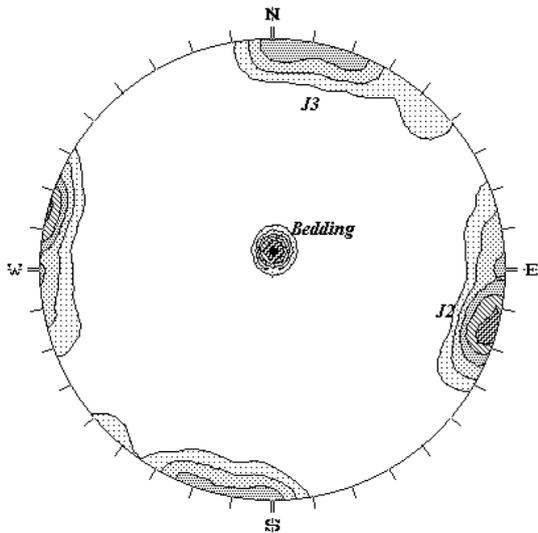
Upper hemisphere projection of poles

Figure 4: Spacing (Top) and orientation (Bottom) of discontinuities at Herod's Palace, Masada.

Strength and Elasticity of Intact Rock

The uniaxial compressive strength of intact rock samples exceeds 315 MPa, and typical values of Elastic modulus and Poisson's ratio are 40 GPa and 0.18 respectively. These strength and elasticity parameters are relatively high with respect to values determined experimentally for other dolomites and limestones in Israel (e.g. Hatzor and Palchik, 1998).

Shear Strength of Discontinuities

The shear strength of filled bedding planes was determined using a segment triaxial test performed on a right cylinder containing an inclined saw cut plane at 35° to the axis of the cylinder, filled with crushed dolomite. Seven different segments were performed, with confining pressure values ranging between 2.2 and 16.2 MPa. A linear Coulomb – Mohr failure criterion was found, with zero cohesion and a residual friction angle of 22.7^o. Identical result was found for tilt tests performed on polished surfaces thus establishing a residual friction angle vlaue of 23° which should be applicable for very large blocks. For dynamic analysis of smaller blocks however, the strengthening effect of initial asperities ought to be considered.

The shear strength of rough bedding planes was determined using real bedding plane samples from the foundations of the palace. The upper and lower sides of the mating planes were kept in contact with no disturbance and were transported to the lab at natural water content. The two samples were cast inside two 200mmX200mmX150mm shear boxes while the mating surfaces were kept intact. The gap between the rock and the box frame was filled with Portland cement.

Direct shear tests were performed using a hydraulic, close loop servo-controlled, direct shear system with normal force capacity of 1000kN and horizontal force capacity of 300kN (Product of TerraTek Systems Inc.). The stiffness of the normal and shear load frames was 7.0 and 3.5 MN/m respectively. Normal and horizontal displacement during shear were measured using four and two 50mm LVDT's with 0.25% linearity full scale. Axial load was measured using a 1,000 kN capacity load cell with 0.5% linearity full scale. Shear load was measured using a 300kN load cell with 0.5% linearity full scale. Two segment direct shear tests were performed (samples MNP3, MNP4) under a constant shear displacement rate of 1mil/sec (0.025 mm/sec) and under an imposed constant normal stress condition. An example of direct shear test result is shown in Figure 5 which also displays a typical failure criterion for the joints:

$$0 < \sigma_n < 0.5\,MPa \; : \tau = 0.88\,\sigma_n\,(R^2 = 0.999\,)$$

$$0.5 < \sigma_n \le 12\,MPa \; : \tau = 0.083 + 0.71\sigma_n\,(R^2 = 0.998\,)$$

This criterion suggest that for low normal stress conditions the peak friction angle on sliding planes is not greater than 41°. This value was used in the dynamic analysis.
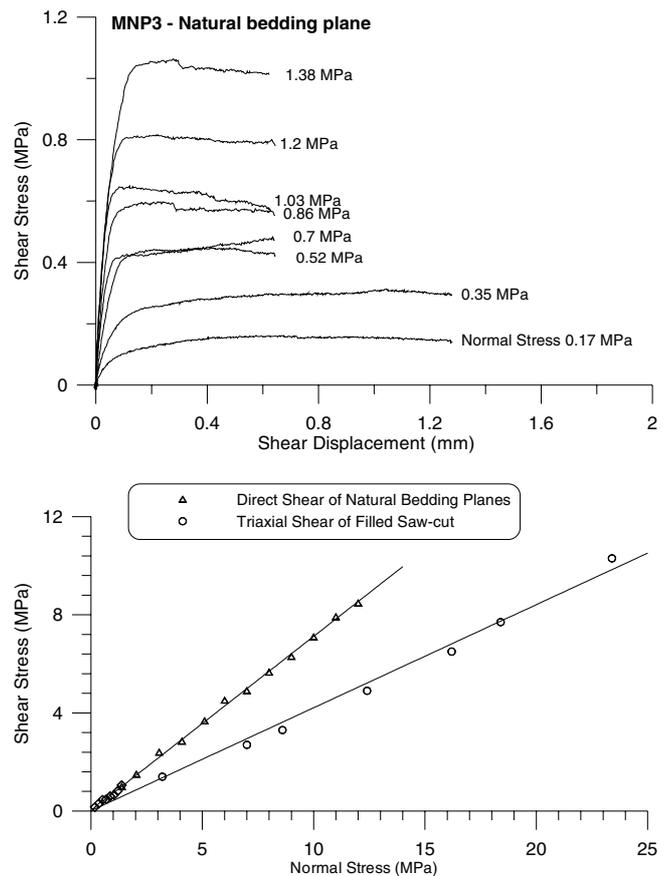

Figure 5: Shear strength of bedding planes. Top - Segment direct shear test, Bottom - Failure envelopes for residual (circles) and peak (triangles) friction angles.

Block System Mesh Generation

The results of numerical analyses are extremely sensitive to: a) the input mechanical and physical properties, b) the geometrical configuration, namely the computed mesh, and c) the input loading function. The geometrical configuration (b) is particularly important in distinct element methods where rock blocks and mesh elements coincide. In the previous section the determination of mechanical parameters was discussed. In this section the most suitable mesh configuration is discussed, followed by a discussion of the appropriate dynamic input motion.

Two principal joint sets and a systematic set of bedding planes comprise the rock structure at Herod's palace (Figure 4). An E-W cross section of the upper terrace is shown in Figure 6, computed using the statistical joint trace generation code (DL) of Shi (1993). It can be seen intuitively that while the East face of the rock terrace is prone to sliding of wedges, the West face is more likely to fail by toppling of individual blocks. Block theory mode and removability analyses confirm these intuitive expectations.
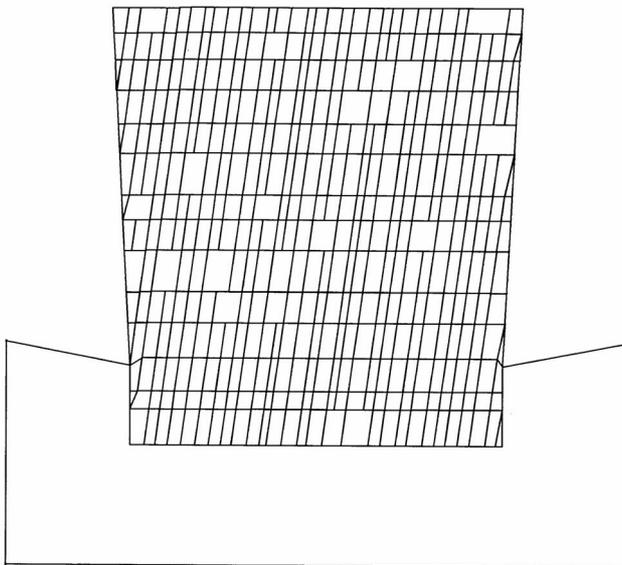
Figure 6: The block mesh using a statistical joint trace generation code (E-W cross section of the upper terrace).

While it is quite convenient to use mean joint set attitude and spacing to generate statistically a synthetic mesh, the resulting product (Figure 6) is quite unrealistic and bears little resemblance to the actual slope. The contact between blocks obtained this way is planar, thus interlocking between blocks is not modeled. Consequently the results of dynamic calculations may be overly conservative and the computed displacements unnecessarily exaggerated. This indeed was the result of several dynamic analysis runs performed in the past for this particular problem.

In order to analyze the dynamic response of the slope realistically a photo-geological trace map of the face was prepared using aerial photographs (Figure 7A), and the joint trace lines were digitized. Then, the block-cutting (DC code) algorithm of Shi (1993) was utilized in order to

generate a trace map that represents more closely the reality in the field (Figure 7B).

Inspection of Figure 7 reveals that block interlocking within the slope is much higher and therefore the results of the forward analysis are expected to be less conservative and more realistic. The deterministic mesh shown in Figure 7 was used therefore in the forward dynamic modelling discussed below.
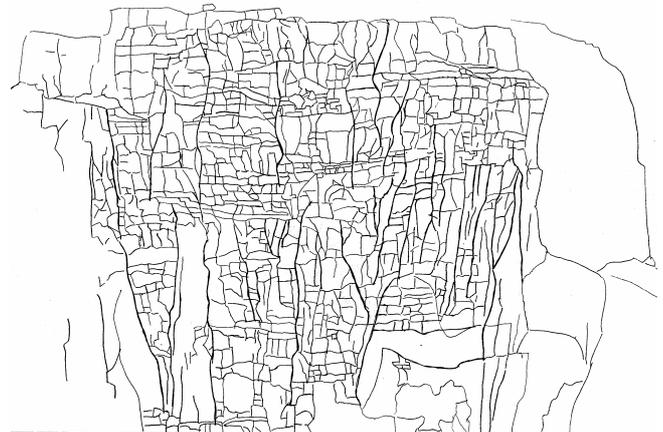
A
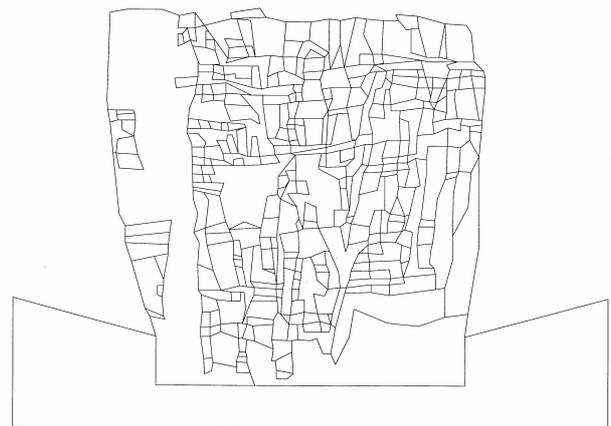
B

Figure 7: Block mesh generation: A) Photo geological trace map, B) Computed block mesh using the geological map and the block cutting algorithm of Shi, 1993.

Input Motions

The significance of the selected input motion

The determination of mechanical input parameters is straight forward in the case of strong and stiff rocks with clean discontinuities as in the case of Masada. The determination of the correct geometrical configuration involves a measure of geological engineering judgment, but nevertheless can be established quite accurately once a sound structural model for the rock mass is put together. The selection of the most suitable input motion for forward dynamic modeling is not a simple task however, as it involves subjective judgment with respect to the most

ISRM 2003 – TECHNOLOGY ROADMAP FOR ROCK MECHANICS

characteristic earthquake for the particular site at hand, and with respect to the relative significance of local site effects.

The Nuweiba earthquake record

In this research we chose to use the recorded time history of the $M_w = 7.1$ Nuweiba earthquake which occurred in November 1995 in the Gulf of Eilat (Aqaba) with an epicenter near the village of Nuweiba, Egypt. The main shock was recorded at the city of Eilat where the tremor was felt by people, and structural damage was detected in houses and buildings. The city of Eilat is located 91 km north from the epicenter and 186 km south of Masada, on the northern coast of the gulf of Eilat (Aqaba). The peak ground acceleration (PGA) of the Nuweiba record as measured in Eilat was 0.09g.

Incorporation of site effects

The Eilat seismological station is situated on a thick fill layer of Pleistocene alluvial fan deposits. The recorded accelerogram therefore represents the response of a site situated on deep fill layer rather than on sound bedrock. Therefore, direct application of the original Eilat record for the case of the Masada rock site would be in appropriate. In order to obtain a "rock response" record for the Nuweiba event it would be necessary to remove the local site effect of the fill layer, which typically amplifies ground motions, and to produce a corresponding "rock" response using an appropriate transfer function. This mathematical procedure is known as de-convolution.

In this research a one-dimensional multi layer model for the fill was utilized (Zaslavsky and Shapira, 2000) with the key parameters being shear wave velocity, thickness, and density for the horizontal fill layers. The material and physical parameters were determined using both seismic refraction survey data and down-hole velocity measurements. The appropriate transfer function was developed by optimization of both theoretical and experimental results.

Although the Masada site is situated directly on rock, a significant topographic effect was recorded in the field (Zaslavsky et al., 2002) and it should therefore be considered in the development of the relevant input motion for the site. An empirical response function for Masada, developed on the basis of the field study discussed above, was found to have three characteristic modes at 1.06, 3.8, and 6.5 Hz. The resulting time history (after convolution) for topographic site effect is shown in Figure 8. The modified Nuweiba record (Figure 8) was used in the forward modelling discussed below.
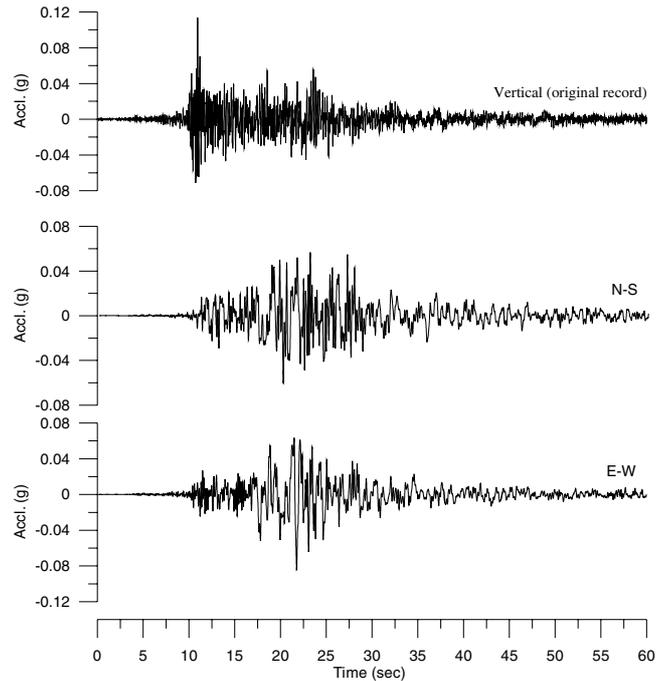

Figure 8: The modified Nuweiba record used for forward dynamic modeling.

Dynamic Analysis

Numerical Control Parameters

The numerical control input parameters for DDA are the energy dissipation parameter (K01), the total number of time steps (n5), the upper limit of time interval used in each time step (g1), the assumed maximum displacement ratio (g2) where (g2)*W is the assumed maximum displacement per time step and W is half the length of the analysis domain measured in the y direction, and the penalty or contact spring stiffness (g0). Hatzor and Feintuch (2001) explored the interrelationships between time step size (g1) and assumed maximum displacement ratio (g2) using comparison between DDA and analytical solutions for dynamic problems (block on an incline subjected to dynamic load). Doolin and Sitar (2002) and Tsesarsky et al. (2002) further studied the role of time step size and penalty value (g0) using comparison with analytical solutions and results of shaking table experiments, respectively. In this research the conclusions from these previous studies are utilized for the selection of the most appropriate input numerical-control parameters, the values of which are listed in Table 1 below. Several comments about the selected time step size (g1) and the energy dissipation parameter (K01) are further discussed below.

Table 1: Numerical control parameters used in forward dynamic modeling

Total number of time steps:	50,000
Time step size (g1):	0.0002 sec.
Maximum displacement ratio (g2):	0.0015
Contact spring stiffness (g0):	$5*10^6$ kN/m
Factor of over-relaxation:	1.3

Time step size

The time step size affects the accuracy and efficiency of the numerical solution (Hatzor and Feintuch, 2001, Doolin and Sitar, 2002, Tsesarsky et al., 2002). For problems with analytical solution the optimal time step size can be determined with great accuracy. Numerical solutions however are used in cases for which analytical solutions do not exist; for such problems the numerical control parameters must be determined in advance on the basis of previous experience and engineering judgment. One way to estimate the suitability of the selected time step size in DDA is to check the average number of iterations per time step (i_{av}) required for convergence.

A high number of iterations per time step (i_{av}) indicates poor convergence rate in each time step. This may adversely affect the accuracy of the solution. For the problem at hand, with a time step size of 0.002 seconds the typical number of iterations per time step was about 9.0, indicating a time step size much too large. With a time step size of 0.0002 seconds however the typical number of iterations per time step was between 2.7 and 3.14, indicating a much better convergence rate and possibly greater accuracy. Therefore, a time step size of 0.0002 seconds was used in all DDA runs presented here.

Note that in preliminary studies of this problem (e.g. Hatzor et al., 2002) the selected time step was set to g1 = 0.002 seconds and a value of n5 = 25,000 time steps was input in order to run the entire 50 seconds event. When the convergence rate is poor however, the DDA code is programmed to cut the time step automatically during the computation (the input value of g1 being only an upper limit). In such cases the actual time computed (ΔT) may be shorter than $g(1) * n5$. This indeed was the case in previous runs of this problem (Hatzor et al., 2002) where the total time computed (ΔT) was typically 15 seconds and not the targeted 50 seconds. With g1 = 0.0002 seconds the total time computed (ΔT) was very close to the 10 seconds target using n5 = 50,000 time steps.

Energy dissipation parameter

DDA formulation is completely linear-elastic with no energy dissipation mechanisms other than the mechanical energy required for elastic deformation of contact springs, elastic deformation of intact block material, and frictional sliding along discontinuities, which is the main source of energy consumption. Consequently, no "artificial" damping is introduced in the mathematical formulation of DDA. While this is an honest approach, it is not entirely realistic because irreversible processes such as crushing of block material at contact points, or temporary resistance to sliding offered by asperities, are not modeled. Such energy dissipation mechanisms, loosely referred to as "damping", must be active during block system deformation and if not modelled, DDA results should be expected to provide exaggerated displacements.

As mentioned above, comparisons between DDA and shaking table experiments for a single block on an incline subjected to dynamic loads proved that with 0% kinetic damping (K01=1) DDA results over predicted block displacements by as much as 80%, while with 2% kinetic damping (K01=0.98) the numerical solution and physical test results converged. The Masada problem presented here consists of 344 individual blocks that interact with one another during dynamic loading. Clearly with no kinetic damping DDA output should be expected to be overly conservative and the predicted damage excessive. The question of exactly how much kinetic damping would be necessary for valid damage prediction in this multi-block case can only be answered by repeated trials and errors. In this research we ran the problem repeatedly for kinetic damping values of: K01 = 1, 0.99, 098, 0.975, 0.95, corresponding to 0%, 1%, 2%, 2.5%, and 5% kinetic damping.

Time window for analysis

Consider the complete 50 seconds record shown in Figure 8. Using the optimal time step size for this problem (0.0002 seconds), a total number of 250,000 time steps would be required to complete the computation of the entire event from t_o = 0 seconds, to t_f = 50 seconds. Such an analysis would take more than a week to complete, even with a fast computer, and would yield an extremely large data output file (approximately 150Mb per a single run), making data handling and processing an elaborate task. Since the value of the selected time step size could not be compromised, we decided to focus the analysis on the 10 most critical seconds in the record, from t_o = 15 seconds to t_f = 25 seconds. Therefore, n5 = 50,000 time steps was used as input to compute the complete 10 seconds time window. The average CPU time per run on a P4-1.5GHz processor with 128Mb RAM was typically 36 hours. The typical size of the data output file for a single run was 28Mb. With the specified time step size of g1 = 0.0002 seconds the total time of the analysis was very close to ΔT = 10 seconds.

Mechanical Input Parameters

The mechanical input parameters were based on the laboratory experiments described above. The joints were assumed cohesionless and with zero tensile strength. The assumed friction angle on all joints was set to 41° based on the direct shear test results that were performed on natural bedding planes. The values of elastic modulus and Poisson's ratio for intact rock material were taken directly from uniaxial compression tests. Table 2 summarizes the selected mechanical input parameters for the analysis.

Table 2: Mechanical input parameter for DDA modeling.

|	
Unit weight of rock (γ):	25 kN/m^3
Elastic Modulus (E):	$43*10^6$ kN/m^2
Poisson's Ratio (ν):	0.184
Friction angle of all discontinuities (ϕ):	41°
Cohesion of all discontinuities (C):	0
Tensile strength of discontinuities (σ_t):	0

Results of dynamic analysis

The critical 10 seconds of the earthquake were computed using the modified rock response record (Figure 8) with different amounts of kinetic damping. The response of the studied terrace to stronger events was studied by normalizing the original record to PGA values of 0.2g, 0.6g, and 1g. The graphical output is shown in Figure 9 and 10 and the meaning of the results is discussed below.
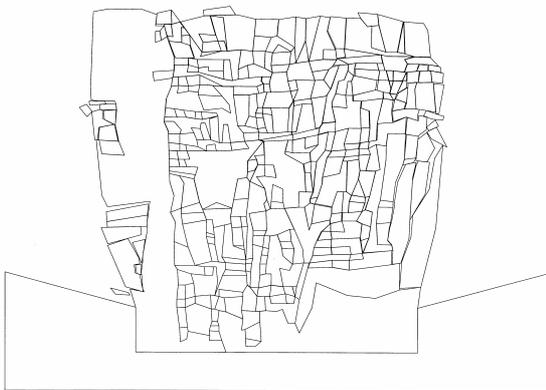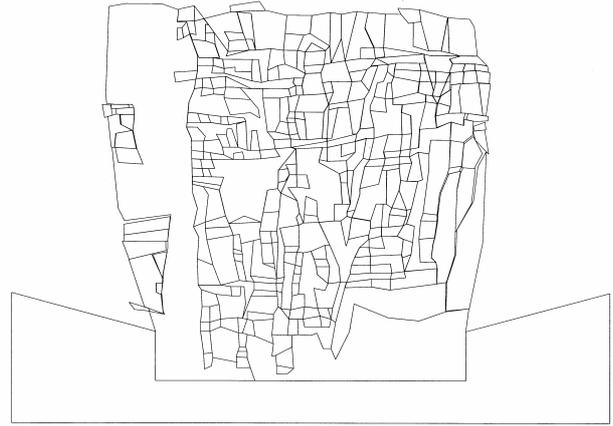
Discussion

Energy dissipation calibration

In Figure 9A the result of DDA computation for the modified rock response record (Figure 8) is shown for time window $t_0 = 15$ to $t_f = 25$ seconds for a computation
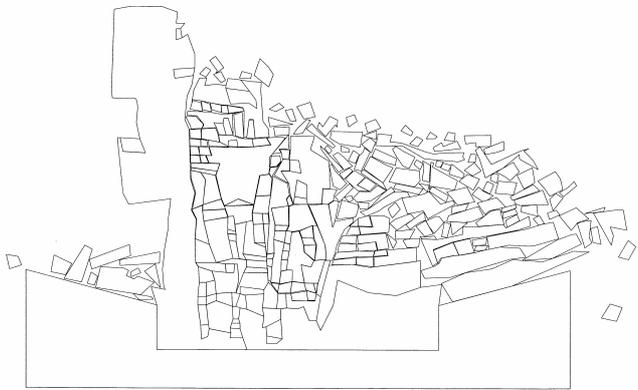
A

B

C

Figure 9: Results of dynamic DDA modeling for the modified Nuweiba record: A) no energy dissipation, B) 2.5% kinetic damping, C) 5% kinetic damping.

with no energy dissipation, or with zero kinetic damping. The resulting damage is devastating and the terrace completely disintegrates. Recall that the peak horizontal ground acceleration (PGA) for the original (modified) record was only 0.06g (Figure 8). On the basis of historical and seismological evidence we believe that the terrace must have been subjected to many events of similar magnitude since Herod fortified it, yet it remained largely intact during its 2000 years of recorded history. Therefore, the damage presented in Figure 9A must be considered excessive and unrealistic. From the output shown in Figure 9A it clearly seems that a certain amount of energy dissipation must be considered to truly simulate the performance of a jointed rock slope subjected to dynamic loading, using DDA.

In Figures 9B the same record is computed but with 2.5% kinetic damping. Introduction of a relatively small amount of energy dissipation drastically reduces the computed damage for the terrace, and with further energy dissipation (Figure 9C) the damage is further restrained.

Judging from the output shown in Figure 9 it does not seem justified to introduce 5% kinetic damping (Figure 9C), since even with 2.5% damping the terrace remains largely intact (Figure 9B). The shaking table validation study showed that with 2% kinetic damping DDA and experimentally obtained displacements converged (Figure 2). The results of the analysis presented here confirm the experimental results and imply that the same amount of energy dissipation should be considered in dynamic DDA calculations for both single and multiple block problems. On the basis of the above discussion the estimated amount of required kinetic damping is believed to be 2%. This value is strictly valid for DDA and it should be determined separately for other distinct element methods.

The influence of rock bolt reinforcement

Modeling bolting reinforcement is straightforward in the DDA method and the implementation of strain energy for bolting connections is discussed in detail by Shi (1993). Yeung (1991, 1993) demonstrated bolting reinforcement for underground problems using DDA and discussed it's

511

potential for general application. In this case two rock bolting configurations are modeled:

Bolt length = 6m, spacing = 2m, stiffness = $24 * 10^4$ kN/m^2, both west and east faces (Figure 10A).
Bolt length = 6m, spacing = 4m, stiffness = $24 * 10^4$ kN/m^2, only west face (Figure 10B).

The modeled bolts were not pre-tensioned. The block mesh with the different bolting patterns was subjected to the modified record normalized for PGA = 0.6g for the same 10 seconds time window used in previous analyses, and with the same time step size of 0.0002 seconds.

The effect of rock bolting is apparent. With the dense bolting pattern the terrace remains virtually intact after 10 seconds of shaking with PGA = 0.6g, and all the blocks remain in place. With the sparse bolting pattern which was limited to the west face only, severe damage is detected in the east face. In the sparsely reinforced west face however only local block failures are detected. The effectiveness of bolting reinforcement in jointed rock masses is evident from the output in Figure 10.
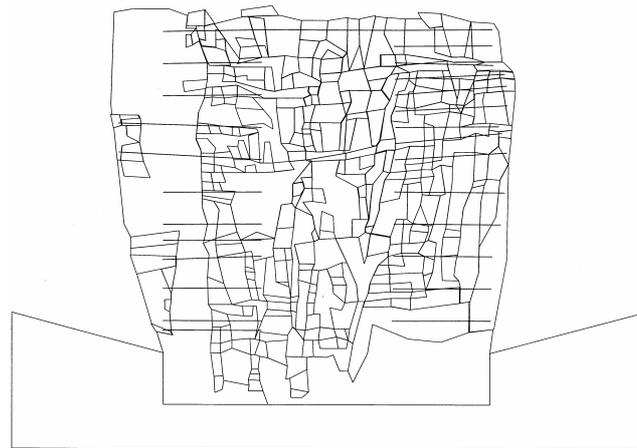
A
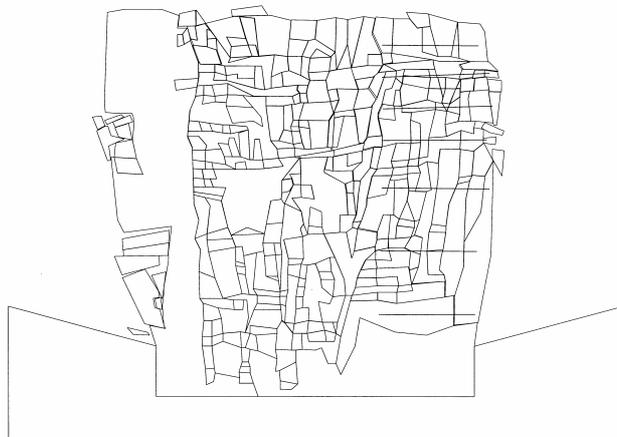
B

Figure 10: Performance of the rock slope with rock blot reinforcement. Modified Nuweiba record with 2% kinetic damping normalized to PGA = 0.6g: A) Dense bolting pattern, B) sparse bolting pattern.

Conclusions

● In order to model dynamic deformation of jointed rock slopes every attempt should be made to determine as accurately as possible the mechanical properties of the rock mass, the geometry of the rock structure, and the expected style of dynamic loading.

● The time step size used in the solution process effects the convergence rate and should be selected carefully. For DDA we find that a small time step size is preferable, even if the total length of the analysis time must be compromised.

● By comparison with historical records we conclude that some energy dissipation must be introduced to the otherwise un – damped DDA formulation. The required amount of kinetic damping seems to be in the order of 2%, based on both shaking table experiments and field scale performance. This value is strictly true for DDA only and must be determined separately for each distinct element code.

● In this research we performed calibration, or fine tuning, of the numerical control parameters by comparison between numerical modelling output and field scale performance. This calibration is un-avoidable, and is required in all other methods as well. However, once the numerical control parameters are calibrated, investigation can proceed with different or more complex problems, utilizing the power of the numerical tool.

● Bolting reinforcement proves to be extremely efficient in stabilization of jointed rock slopes that are subjected to dynamic loads.

Acknowledgements

References

BEN – MENAHEM, A. Earthquake Catalog for the Middle East. Bollettino di Geofisica Teorica e Applicata, v. XXI, pp.245-313. 1979.

DOOLIN, D. M. and SITAR, N. Displacement accuracy of Discontinuous Deformation Analysis method applied to sliding block. Journal of Engineering Mechanics. Vol. 128, No. 11, pp. 1158 – 1168, 2002.

HATZOR, Y. H. and V. PALCHIK. A microstructure-based failure criterion for Aminadav dolomites - Technical Note. International Journal of Rock Mechanics and Mining Sciences, Vol. 35, No. 6, pp. 797-805, 1998.

HATZOR, Y. H. and FEINTUCH, A. The validity of dynamic displacement prediction using DDA. International Journal of Rock Mechanics and Mining Sciences. Vol. 38, No. 4, pp. 599-606. 2001.

HATZOR, Y. H., ARZI, A. A. and TSESARSKY, M. Realistic Dynamic Analysis of Jointed Rock Slopes using DDA. Stability of Rock Structures: Proceedings of the 5th International Conference of Analysis of Discontinuous Deformation (ed. Y. H. Hatzor), Balkema Publishers, Lisse, pp. 47 – 56. 2002.

MCBRIDE, A., and SCHEELE, F. Investigation of discontinuous deformation analysis using physical laboratory models. Proceedings of ICADD-4, 4th International Conference of Analysis of Discontinuous Deformation (N. Bicanic Ed) Glasgow, Scotland, UK. 2001.

NETZER, E. Masada III – the Yigael Yadin Excavations 1963-1965 Final Reports – The Buildings Stratigraphy and Architecture. Israel Exploration Society, The Hebrew University, Jerusalem, Israel, 665p. 1991.

NIEMI, T. M., Z. BEN AVRAHAM and J.R. GAT (Editors),. The Dead Sea, The lake and its setting. Oxford Univ. Press Ltd., 286pp, 1997.

SHAPIRA, A. and VAN ECK, T.. Synthetic uniform hazard site specific response spectrum, Natural Hazard, 8:201-205. 1993.

SHI, GEN-HUA. Block System Modelling by Discontinuous Deformation Analysis, Computational Mechanics Publications, Southampton UK, p. 209., 1993.

SHI, GEN-HUA. Single and multiple block limit equilibrium of key block method and discontinuous deformation analysis. Stability of Rock Structures: Proceedings of the 5th International Conference of Analysis of Discontinuous Deformation (ed. Y. H. Hatzor), Balkema Publishers, Lisse, pp. 3 – 43. 2002.

TSESARSKY, M., HATZOR, Y. H. and SITAR, N. Dynamic block displacement prediction – validation of DDA using analytical solutions and shaking table experiments. Stability of Rock Structures: Proceedings of the 5th International Conference of Analysis of Discontinuous Deformation (ed. Y. H. Hatzor), Balkema Publishers, Lisse, pp. 195 – 203. 2002.

WARTMAN, J. Physical model studies of seismically induced deformation in slopes. Ph.D. Dissertation, Dept. of Civil and Env. Engrg, University of California, Berkeley. 1999.

YEUNG, M. R. Application of Shi's Discontinuous Deformation Analysis to the study of Rock Behavior. Ph.D. thesis, University of California, Berkeley. 1991.

YEUNG, M. R.. Analysis of a mine roof using the DDA method. International Journal of Rock Mechanics and Mining Sciences, Vol. 30, No. 7, pp. 1411-1417. 1993.

ZASLAVSKY, Y. and SHAPIRA, A. Questioning nonlinear effects in Eilat during M_W=7.1 Gulf of Aqaba Earthquake, Proceeding of XXVII General assembly of the European Seismological Commission (ESC), Lisbon, Portugal, September 10-15, 343-347, 2000.

ZASLAVSKY Y, A. SHAPIRA and A.A. ARZI. Earthquake site response on hard rock - empirical study. Stability of Rock Structures: Proceedings of the 5th International Conference of Analysis of Discontinuous Deformation (ed. Y. H. Hatzor), Balkema Publishers, Lisse, pp. 133 – 144. 2002.

ISRM 2003 – TECHNOLOGY ROADMAP FOR ROCK MECHANICS